Petroleum and Coal

Article **Open Access**

Modelling of Drillstring Hook Loads for Torque and Drag Evaluation in Extended Reach Wells

Ubanozie Julian Obibuike, Stanley Toochukwu Ekwueme, Nnaemeka Princewill Ohia, Frank Chinedu Ukaeru, Ifeanyi Michael Onyejekwe, Mathew Chidubem Udechukwu, Hassan Babidi Yahya*

Department of Petroleum Engineering, Federal University of Technology, Owerri, Nigeria

Received March 14, 2025; Accepted June 22, 2025

Abstract

Accurate estimation of Hookload (HKL) is crucial for preventing critical drilling challenges such as drill line failure, rig instability, drillstring parting, and helical buckling. This study employed WellPlan software to model drillstring torque and drag under varying operational scenarios, with an emphasis on HKL behavior in extended reach wells. Torque and drag analyses focused on tripping in and tripping out operations. Sensitivity analyses assessed the effects of mud weight, open-hole friction factor, tripping speed, and rotary speed (RPM) on HKL. Additionally, Response Surface Methodology (RSM) with Box-Behnken Design (BBD) was utilized to develop predictive models and analyze interaction effects among these parameters. Results showed that mud weight and friction factors significantly impact HKL. Higher mud weight lowers HKL by increasing buoyancy, whereas higher friction factors raise HKL during tripping out but decrease it during tripping in. Tripping speed and RPM also affect HKL due to dynamic surge and swab pressures. RSM demonstrated excellent predictive capability: the quadratic model best represented tripping in data, while the linear model was optimal for tripping out. For tripping out, the R^2, adjusted R^2, and predicted R^2 values were 0.9766, 0.9727, and 0.9634, respectively; for tripping in, these were 0.9828, 0.9656, and 0.9010.. ANOVA and fit summary confirmed statistical reliability, with minimal discrepancies between predicted and actual values. These results highlight RSM's strong predictive capability, offering a robust framework to analyze how key parameters affect HKL. This work supports safer and more efficient tripping, enhanced load management, and mitigation of risks such as buckling and drillstring failure in extended reach drilling operations.

Keywords: *Hook loads; Torque and drag; RSM; ANOVA; Tripping; Drillstrings; Extended reach wells.*

1. Introduction

Directional drilling has significantly transformed oil and gas well engineering, marking a major technological shift that has enabled complex well configurations, including highly deviated wells and maximum reservoir contact (MRC) wells. This evolution in drilling technology facilitates the development of horizontal, multilateral, and extended reach wells (ERWs) [1-2]. These advanced well designs offer considerable advantages over traditional vertical wells by boosting productivity, enhancing sweep efficiency, expanding drainage areas, and lowering the cost per barrel produced [3-4]. However, as wellbore trajectories become more intricate, casing installation grows more challenging—especially in ERWs, where extended horizontal sections and high deviation angles introduce notable risks [5].

Extended reach wells, often termed long-reach wells, are characterized by lateral departures that frequently exceed the true vertical depth (TVD) [6]. By increasing horizontal exposure to the reservoir, ERWs aim to maximize recovery, but this also brings significant drilling challenges [7]. Critical factors like high dogleg severity, greater mechanical stresses, elevated torque and drag, and wellbore stability must be rigorously addressed to ensure

successful casing installation and sustained well integrity [8]. Of particular concern is torque and drag management, as these forces are intensified in ERWs and directly impact wellbore stability and cementing operations [6].

Torque and drag pose persistent challenges throughout downhole operations, including tripping, sliding, and drilling activities for both construction and maintenance phases [9]. Excessive torque and drag increase the risks of buckling and string wear and heighten the probability of stuck pipe or lockup, which may demand costly fishing operations or lead to well abandonment in severe cases [10]. Unchecked, these issues can cause significant financial losses, with industry reports showing that unresolved torque and drag problems cost millions annually [7].

Modern complex well paths, especially in ERWs, require early and accurate torque and drag modelling during the design stage. Such modelling helps engineers optimize the configuration of downhole strings and bottom hole assemblies (BHAs), improving well integrity and minimizing mechanical failures [11]. Precise estimates bridge the gap between simulations and actual conditions, reducing unexpected complications [12-13]. In ERWs, the extended lateral reach increases the contact area between the drillstring and borehole wall, amplifying friction and raising torque and drag, especially in horizontal sections [14]. A key parameter for managing torque and drag in ERWs is the hook load (HKL), which acts as an axial load indicator influencing drillstring frictional resistance [15]. Accurate hook load readings are vital for determining the weight on bit (WOB) and diagnosing issues like severe tortuosity, poor hole cleaning, or high friction that contribute to elevated torque and drag. Variations in hook load highlight zones with excessive drag, signaling potential drilling hazards [15].

However, hook load data can be prone to uncertainties since it is typically measured indirectly via tension in the travelling equipment or dead line [15]. This apparent hook load can be distorted by additional forces such as the mud hose weight, sheave tension variations, and dynamic forces acting on the drill line. These extraneous effects can mask the actual hook load, causing inaccuracies in torque and drag estimations. Correcting for such factors is vital to ensure hook load readings truly reflect the drillstring's axial force, supporting more precise control [15].

Reliable hook load measurements are also essential for mitigating risks linked to overpull and excessive drill line strain. High hook load can lead to dangerous failures such as parting the drill line, pulling the rig inward, or snapping the drillstring [16]. These risks often arise when overpull from the drawworks misinterprets the actual cable tension in the block-and-tackle system. Inaccurate hook load data increases the chance of incorrect WOB adjustments, potentially overstressing the drawworks fast line and causing unexpected failures [17]. Improving hook load accuracy requires careful modelling and compensation for external forces acting on the drill line [15]. Such refinements give operators a clearer understanding of downhole mechanics, allowing better adjustments to WOB and helping prevent mechanical issues [16]. This proactive, data-driven approach is essential for controlling drilling dynamics, especially in demanding ERW operations, where precise torque and drag management is critical for safe and efficient well delivery.

2. Literature review

2.1 Hook loads in torque and drag evaluation

The hook load is a critical parameter in drilling operations, representing the vertical force acting on the elevator or top-drive shaft at the top of the travelling equipment as it supports the drill string. It is affected by multiple forces, including the submerged string weight and the mechanical and hydraulic friction forces encountered during drilling [18]. By reflecting the combined effect of these forces in the wellbore, the hook load serves as a key variable for understanding downhole conditions, frictional resistance, and overall drilling dynamics [19].

A primary contributor to hook load is the drag force from friction between the drill string and the wellbore wall. This drag depends on contact points along the string, wellbore geometry (curvature, tortuosity), and the type of drilling fluid used [20]. As the string moves, friction

accumulates, forming a significant portion of the measured hook load. Additionally, pressure forces from buoyancy, fluid flow inside the string, and fluid shear at the pipe walls affect weight distribution and hook load. Together, these factors make the hook load a vital indicator for monitoring drilling efficiency and diagnosing downhole issues [17].

Operators routinely use hook load readings to estimate the weight on bit (WOB), a key factor for controlling drilling rate and avoiding bit wear or inefficiency. By tracking the hook load, operators can infer bit weight and adjust parameters to optimize drilling [7]. Fluctuations can also signal changes in downhole conditions, like increased friction or stuck pipe risk, allowing timely responses. Therefore, precise hook load measurement is crucial for managing mechanical friction, efficient weight transfer, and minimizing excessive torque and drag [15].

In drilling, the hook load acts as an indirect yet essential diagnostic tool for assessing the wellbore's condition and drill string dynamics. Changes in hook load can indicate issues such as wellbore instability, diameter changes, excessive tortuosity, or signs of stuck pipe [18,21]. For example, a rising hook load may mean higher friction due to borehole narrowing, while a drop could signal reduced bit contact with the formation.

This measurement is especially important in torque and drag modelling for complex well paths like extended reach wells (ERWs), where longer lateral sections cause significant frictional forces. Accurate hook load monitoring and adjustments help avoid problems such as string lock-up, buckling, or stuck pipe [19]. Real-time monitoring enhances operational safety and drilling efficiency in these demanding environments.

It is possible to directly measure the true hook load at the top of the drill string using an instrumented Internal Blow-out Preventer (IBOP) as discussed by Wylie *et al.* [22]. This method offers precise, real-time axial force readings but is not yet widely implemented. Currently, only select top drives have this capability, so most rigs still rely on indirect estimation methods [8,24].

On rigs lacking advanced sensors, the hook load is typically measured indirectly with a load cell at the top drive's hanging point or by measuring tension in the dead line of the draw-works system. While common, these methods have limitations [15]. Indirect readings can be distorted by forces unrelated to axial string tension, such as the mud hose weight, tension variability across sheaves, and gravitational and inertial effects from drill line weight and rotation [15].

Such extraneous forces can cause the apparent hook load to deviate from the true axial force, leading to inaccurate assessments that may compromise operational decisions during drilling [25]. To address this, correction methods are essential to filter out unrelated loads and isolate the actual hook load. Without proper corrections, operators risk making poor WOB adjustments, increasing the chance of excessive friction or mechanical failures [26].

By integrating correction factors into indirect measurement techniques, engineers can more accurately interpret the hook load, improving their ability to monitor well conditions, optimize drilling, and avoid problems like stuck pipe or instability [27]. Reliable hook load data remains vital for safe and efficient rig operations, especially in complex wells such as ERWs where downhole dynamics must be carefully controlled [7].

Modelling the interaction between inputs and resulting hook load is complex due to the non-linear behaviour of torque and drag. Statistical methods like Response Surface Methodology (RSM) help model these interactions efficiently. RSM assesses how responses depend on independent variables and their interactions [28]. This technique reduces experimental runs, saving time and cost. Using regression analysis within defined ranges, RSM finds optimal variable combinations for the best outcomes, making it a powerful tool for optimizing complex, multi-variable processes [29-30].

2.2. Common operations in torque and drag and the impact of hook load

Various drilling and completion operations directly influence torque, drag, and consequently the hook load, which is critical for assessing forces acting along the drill string. When tripping in, the drill string is lowered into the wellbore without rotation, creating axial motion with drag forces but no torque. This drag force is negative because the string moves against gravity [26], reducing the apparent weight and resulting in a lower hook load than the true submerged string weight. Accurate measurement ensures the hoisting system handles this safely [31].

Conversely, during tripping out, the string is pulled upward in line with gravity. Here, the drag force is positive and adds to the buoyed weight, increasing the hook load above the static submerged weight, so monitoring is crucial to avoid overstressing equipment and to maintain safe handling [31].

In rotating-on-bottom drilling, the string and bit rotate at the well's bottom to cut the formation while axial movement is minimal. The hook load reflects the weight on bit (WOB) combined with axial string forces. Proper monitoring keeps bit force optimal, prevents excessive torque, and reduces stuck pipe or wear risks [32]. During sliding, mainly used for deviated or horizontal sections, the string moves axially with limited rotation via a mud motor [7]. Hook load indicates both axial force and friction from restricted rotation; increased wall contact raises drag, so close observation helps prevent sticking or high torque [31].

Reaming enlarges or cleans the hole while rotating and circulating fluid. This adds torque and drag, so the hook load shows axial load plus drag from the reamer and pipe contact; careful monitoring prevents overload or stuck pipe [33]. Back-reaming happens when the drill string is pulled out while rotating, but the bit is not cutting rock [7]. This upward motion with rotation adds drag and torque, raising the hook load. Without careful monitoring, it can overstress the hoisting system and cause sticking or lockup [34]. Understanding this helps crews manage weights, control torque and drag, and keep drilling safe and efficient.

3. Method

The method considered in this study comprises the simulation and optimization of Hook load. Hook load was simulated for tripping in and tripping out operations from the torque and drag module in WellPlan software. Sensitivity analyses were conducted on the effect of input parameters that affect the HKL results. These parameters included the mud weight, the openhole friction factor (OHFF), the tripping speeds and the tripping rotary speeds (RPM). Design Experts software was then used to design a experiment using the BBD design of experiment which enabled the determination of sensitivity dataset from the WellPlan utilized to mode the interactions between the HKL and the input parameters using response surface methodology (RSM).

3.1. Case study

The case considered is a drilling operation on Well AB13 in Asa field in the Niger Delta. The planned well trajectory depicts an extended reach drilling. The well depth is 35017 ft drilled across several sections. The section of the well drilled is the production hole which comprises 8-1/2 inch hole and comprises of 22,867 ft length of well and ranging from 12,150 ft to 35,017 ft of measured depth. The upper sections of the well comprises the conductor pipe (30 in casing) from surface to 400 ft of measured depth, surface casing (13-3/8 in casing) from 400 ft to 6,102 ft of MD and intermediate casing (9-5/8 in casing) from 6,102 ft to 12,015 ft of MD.

3.2. Data input

The data used for the simulation comprises the following, Survey data or well trajectory (MD, inclination, azimuth), Hole data, Rig data (block weight, number of strung lines), Fluid data, Friction factors, Pore pressure and fluid gradient, Tortuosity data, and Operations data (Tables 1-3).

Table 1. General data.

S/N	Parameter	Value
1	Fluid density (base)	10.8 ppg
2	Block weight	90 kips
3	Block rating limit	1500 kips
4	Friction factors	0.25 OHFF/1.5CHFF
5	Total Well depth	35,017 ft
6	Section of Well under investigation	From 12,015 ft to 35,017 ft
7	Reservoir temperature	220oF
8	Geothermal gradient	1.74oF/100ft

S/N	Parameter	Value
9	Trip speed	60 ft/min
10	Slack-off weight (sliding)	20 kips
11	Maximum yield of Overpull	90%
12	Rheological model	Herschel-Bulkley

Table 2. Hole and casing data.

S/N	Parameter	Value
1	Conductor pipe	30 in OD, 28.5in ID, 234ppf, runs from surface to 400ft
2	Surface casing	13-3/8 in OD, 12.415 in ID, 68ppf, runs from 400ft to 6102 ft
3	Intermediate casing	9-5/8 in OD, 8.535 in ID, 53.5ppf, runs from 6102 ft to 12,150 ft
4	Hole section	8-1/2 in Hole runs from 12,150 ft to 35,017 ft

Table 3. BHA data.

S/N	Type	Length		Body		Weight
		Pipe	Total	OD	ID	
		[ft]	[ft]	[in]	[in]	[lb/ft]
1	8.5'' PDC Bit	1.05	1.05	6.00	2.25	85.0
2	PD 675 Orbit AA 8-1/2'' Stabilized CC (8-3/8'') (w.NP FV)	14.05	15.10	6.72	4.2	105.08
3	Receiver	5.29	20.39	6.86	3.125	100.80
4	EcoScope (LWD)	25.95	46.34	6.813	5.125	141.11
5	Telescope 675 NF	27.11	73.45	6.813	5.125	141.11
6	Stethoscope 675 w/8 1/4 '' Stabilizer	33.03	106.48	6.9	2.81	76.92
7	8-3/8 Reaming Stab (Bi-directional)	5.31	111.79	6.81	2.81	67.64
8	6.75'' Flex NMDC	29.03	140.82	6.75	2.875	106.91
9	Float Sub (with Non-ported float valve)	2.83	143.65	6.75	2.75	117.43
10	6.75'' DH Filter Sub	5.61	149.26	6.75	3.00	106.91
11	6-3/4'' DAV Catcher Sub	13.11	162.37	6.75	2.75	102.73
12	6-3/4'' DAV Valve Sub	6.53	168.9	6.688	2.75	102.73
13	X.O	3.72	172.62	6.87	2.75	109.82
14	3 x 5-1/2'' HWDP (3 joints)	93.68	266.30	5.5	3.25	73.5
15	X/O (VF50 P x 41/2 IF B)	3.64	269.94	7.00	2.875	117.43
16	Jar	30.32	300.26	6.5	2.75	90.88
17	X/O (41/2 IF P x VF50 B)	3.84	304.10	7.00	2.875	117.43
18	9 x 5-1/2'' HWDP (9 joints)	281.22	585.32	5.5	3.25	73.5
19	5-1/2'' IEU x 21.9 lbs/ft VAM® X-Force TM VF50 135	31	616.32	5.5	4.778	21.90

3.3. Model simulation

The torque and drag simulation was conducted in WellPlan software by following a systematic approach to inputting data and configuring parameters. The process began with creating a new project case in WellPlan, which established the scope and objectives of the simulation. This setup allowed for the input of essential data across the software's various editors. The first step after project creation involved specifying the datum and location data for the well. Here, the elevation and field type were entered, modelling the well as an onshore location. These initial settings established the elevation reference point for all subsequent depth measurements.

The next critical component was defining the wellpath. This involved entering key trajectory parameters, such as measured depth (MD), inclination, and azimuth, into the wellpath editor. With these parameters in place, the tortuosity configuration followed. Tortuosity, which represents deviations from an ideal path, was added to the planned trajectory to replicate the

rippling effects of real-world well paths. This was achieved by entering tortuosity data and selecting a suitable tortuosity model, resulting in a more realistic approximation of the wellpath.

With the trajectory established, the simulation proceeded to specify the hole section data. In the hole editor, details of both the cased-hole and open-hole sections were entered. For each section, outer diameter (OD), inner diameter (ID), weight per foot (ppf), depth intervals, and friction factors were provided. Specifically, the conductor pipe, surface casing, and intermediate casing sections were defined, each with respective dimensions, depth ranges, and cased-hole friction factors (CHFF). The open-hole section was configured with multiple open-hole friction factor (OHFF) values for sensitivity analysis, allowing the model to examine the effects of variable friction on torque and drag.

The simulation then moved to configuring the downhole strings and the Bottom Hole Assembly (BHA) within the string editor. Here, each component's dimensions and mechanical properties were specified, including OD, ID, length, weight, material grade, yield strength, Poisson's ratio, burst and collapse pressures, and torque ratings. This detailed setup allowed for accurate modelling of the drill string dynamics, ensuring that all parameters affecting torque and drag were accounted for in the analysis.

Fluid properties were then defined in the fluid editor, where the selected where a 10.8 ppg mud was used with a Herschel-Bulkley model which was characterized by its density, shear stress, and shear rate values. These fluid characteristics are critical for computing the frictional drag along the wellbore. Following this, subsurface data were entered into the subsurface editor, where the pore pressure and fracture gradient for the reservoir were specified. Additionally, a geothermal gradient was configured by setting a surface temperature of 90°F and a true vertical depth (TVD) temperature of 220°F, which allowed WellPlan to calculate the temperature effects downhole.

With the subsurface parameters defined, the rig data were then entered in the rig editor. This included the rig-specific parameters, such as block weight, set to 1,500 klbs, and a torque rating of 90,000 ft-lbs. Accurate rig data is essential for calculating hook load and determining safe operational limits for torque. In the operations parameters section, torque and drag operations were configured, specifying tripping in and tripping out activities to evaluate the effect of these operations on hook load. This setup allowed the simulation to assess hook load variation across different operational scenarios, aiding in a deeper understanding of downhole conditions and the drill string's response.

The analysis settings for torque and drag modelling were then configured. This included finalizing parameters such as block weight and selecting the modelling approach, whether stiff string or soft string, based on the drill string's flexibility and wellbore contact points. Sensitivity analysis was subsequently conducted to explore how variable factors impacted hook load results. This included adjustments to friction factors, with base values set to 0.15 (CHFF) for the cased-hole and 0.25 (OHFF) for the open-hole sections, as well as variations in mud weight, tripping speed, and rotational speed (RPM) during tripping operations. These sensitivity tests enabled the assessment of how changes in input variables influenced drag forces, buoyancy effects, and torque under different operational conditions.

Once all data were entered, the simulation was executed, and the results from the torque and drag module were analyzed. The base case provided initial hook load values, while the sensitivity analyses offered insights into how adjusting factors like mud weight, friction, and tripping speed affected the results. This comprehensive approach in WellPlan allowed for an accurate representation of torque and drag behaviour, aiding in optimizing drilling operations by providing data on operational adjustments that can reduce drag and prevent overloading of the drill string. This structured process ensures that all critical elements of the simulation are accounted for, enabling effective modelling of torque and drag forces in a range of operational contexts.

The formula for Hookloads for a section is given as

$$HL = \sum_{i=1}^{n} (W_{bt} \cos\theta) + W_{block} \qquad (1)$$

where, W_{bt} = Bouyed wight of string for that section, Lbs; W_{block} = weight of traveling block.

3.4. Sensitivity analyses

Sensitivity analyses were performed to assess the impact of the sensitive input parameters on the Hook load (HKL) result. Parameters including the mud weight, the openhole friction factor, the tripping speed and the tripping rotary speed were assessed. Table 4 gives the values of the sensitivity analyses for the parameters considered.

Table 4. Sensitivity analyses values.

Parameters	Values
Mud weight	9.6ppg to 10.8 ppg
OHFF	0.2 to 0.35
Tripping speed	40 ft/min to 80 ft/min
Tripping rotary speed	O to 20 RPM

3.5. RSM modelling

The sensitivity results obtained from drilling simulation software were used as data for RSM modelling. A Box-Behnken design (BBD) was employed to design the experimental plan using Design Experts, chosen for its effectiveness in modelling complex response surfaces typical of torque and drag.

The implementation of RSM modelling starts with designing the experiments. After designing the experiments, they are executed or simulated under predefined conditions. Following this, various models are applied, and the process involves selecting the most appropriate and accurate model. This selection is determined through thorough analysis, including Analysis of Variance (ANOVA) and fitness parameters. Once the optimal model is identified, the optimization phase begins. This phase focuses on refining system parameters to achieve the best possible outcomes based on the insights provided by the selected model. The flowchart for the RSM model is given in Figure 1.

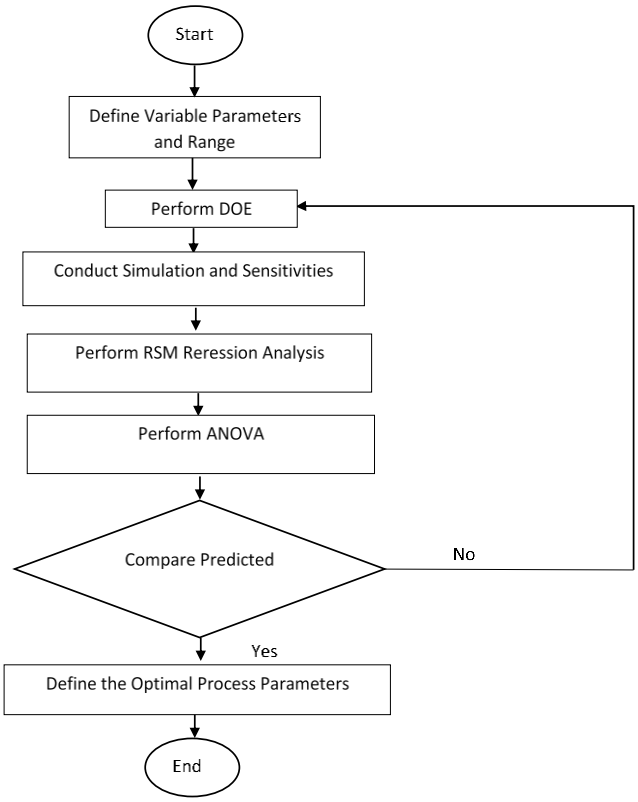

Figure 1. Flowchart for RSM modelling.

The study investigated four variables including mud weight, OHFF, the tripping speed and the tripping rotary speed, known to influence HKL. A total of 29 experimental runs were generated by the BBD for modelling purposes. Various regression analysis models were evaluated to identify the most accurate model fitting the experimental data. Model selection criteria included statistical parameters such as R-squared (R^2), adjusted R-squared, predicted R-squared, standard deviation, and coefficient of variance (COV). Multiple regression analyses facilitated the fitting of these models to the experimental data, allowing for the estimation of responses from independent variables using the following general equations:

The general form of the models for linear regression is given as

$$y = a_o + \sum_{i=1}^{k} a_i x_i + e \qquad (2)$$

The general form of the 2FI regression model is given as

$$y = a_o + \sum_{i=1}^{k} a_i x_i + \sum_{i<j}^{k} a_{ij} x_i x_j + e \qquad (3)$$

The general form of the quadratic regression model is given as

$$y = a_o + \sum_{i=1}^{k} a_i x_i + \sum_{i<j}^{k} a_{ij} x_i x_j + \sum_{i=1}^{k} a_{ii} x_i^2 + e \qquad (4)$$

where x_i,x_j, x_l, are the input variables and a_i, a_{ij}, a_{ii},and a_{ijl} are the coefficient of each of the terms; a_o is the offset and e is the residual or error term.

4. Results

The results of the simulations performed are presented in this section. these comprise the simulation results from WELLPLAN, and the result from RSM modelling and simulation.

4.1. HKL Base case result

Figure 2 shows the Hook load plot for stiff string model for the simulation performed at base case conditions

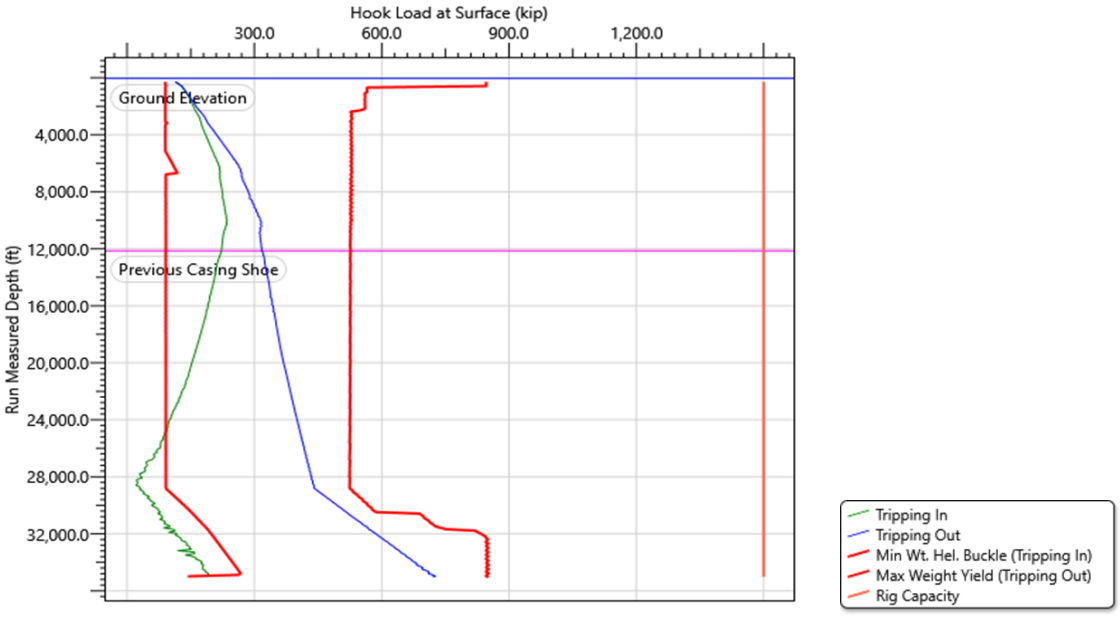

Figure 2. Hook loads for stiff string model.

Figure 2 illustrates the variation in Hook load (HKL) for different operations including tripping in, tripping out, at an open-hole friction factor (OHFF) of 0.25 and a cased-hole friction factor (CHFF) of 0.15. The behaviour of the HKL during these operations reveals significant insights into the interaction between friction and operational loads.

It is evident from the plot that the HKL during tripping out is consistently higher than that during tripping in. This disparity arises because, during tripping out, drag acts in the same direction as the load, thereby increasing the overall HKL. Conversely, during tripping in, the drag opposes the load, leading to a reduction in the HKL. This relationship underscores the role of friction in modifying the mechanical behaviour of the drillstring during these operations.

Two critical thresholds are discernible in the HKL plots. The first is the minimum weight helical buckling (tripping in) line, which defines the lower limit of the HKL during tripping in. If the HKL line intersects this threshold, there is a risk of helical buckling occurring in the drillstring at the regions where the intersection occurs. As seen in the plot, the HKL line during tripping in touches the minimum weight helical buckling line, indicating the potential onset of helical buckling. Helical buckling can lead to increased torque and drag, compromising the efficiency and safety of drilling operations. This observation suggests that careful monitoring and management of tripping loads are crucial to prevent buckling, especially under high-friction conditions.

The second threshold, the maximum weight yield (tripping out) line, represents the upper limit of the HKL during tripping out. If the HKL line crosses this threshold, the drillstring is at risk of yielding or parting, which could result in severe operational failure. In the analyzed case, the HKL line does not intersect the maximum weight yield line for the OHFF of 0.25, indicating that the risk of string parting during tripping out is minimal under the specified conditions. This result highlights the adequacy of the operational parameters in maintaining the structural integrity of the drillstring during tripping out.

4.2. Effect of mud weight on the Hook load

Mud weight was shown to have impact on the HKL related to the buoyant and hydrostatic forces in the wellbore. The effect of mud weight on the HKL is illustrated in Figure 3. the mud weight was varied between 9.6 ppg and 10.8 ppg using Herschel-Bulkley model.

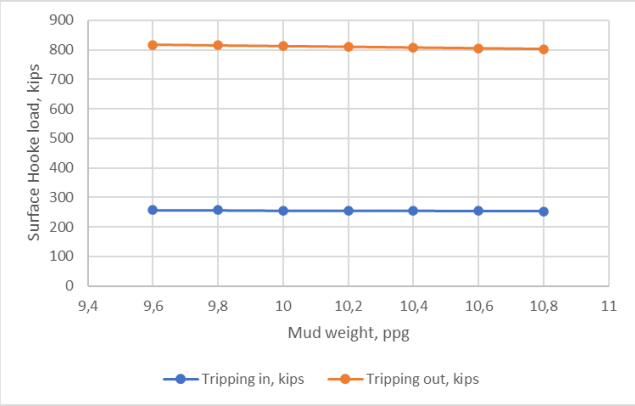

Figure 3 demonstrates the influence of varying mud weight on Hook load (HKL) during tripping in and tripping out operations. The results reveal that increasing the mud weight leads to a slight reduction in the corresponding HKL values for both operations. This behaviour can be attributed primarily to the effect of buoyancy, which plays a crucial role in altering the apparent weight of the drillstring.

Figure 3. Effect of mud weight on the HKL.

When mud weight is increased, the buoyancy force acting on the drillstring also increases. This increased buoyancy reduces the apparent weight of the drillstring in the liquid-filled wellbore, thereby decreasing the axial force required to support or move the string. As a result, the HKL decreases with increasing mud weight. Specifically, the reduction in HKL is more pronounced during tripping out operations, where the lifting force required to overcome the weight of the drillstring is directly affected by the buoyancy. This highlights the effectiveness of increasing mud weight as a strategy to reduce the mechanical effort and loads during tripping operations.

In addition to buoyancy, mud weight introduces viscous drag due to the hydrostatic forces acting on the drillstring. While these forces are generally negligible under moderate conditions, they become significant at higher mud weights. Viscous drag exerts opposing effects on HKL depending on the operation: it tends to increase the HKL during tripping out and decrease it

during tripping in. However, the buoyancy effect dominates in most practical scenarios, ensuring that the overall trend is a reduction in HKL as mud weight increases.

Quantitative analysis of the results reveals that a 0.2 ppg increase in mud weight leads to an approximate 0.3% decrease in the HKL. This relationship highlights the sensitivity of HKL to variations in mud weight and emphasizes the potential for optimization by carefully adjusting mud properties. The observed trend also provides valuable insights for designing efficient tripping operations, as it suggests that moderate increases in mud weight can significantly reduce the mechanical stresses experienced by the drillstring.

4.3. Effect of friction factors on the HKL

The friction factor is critical as the drillstring makes movement in the wellbore. Notably, friction acts to oppose the movement of the strings in the wellbore. As the strings makes contact with the walls of the wellbore, the effect of friction factor becomes apparent influenced by the well geometry, mud properties and operating conditions of the well. The effect of openhole friction factor (OHFF) on the HKL is illustrated in Figure 4.

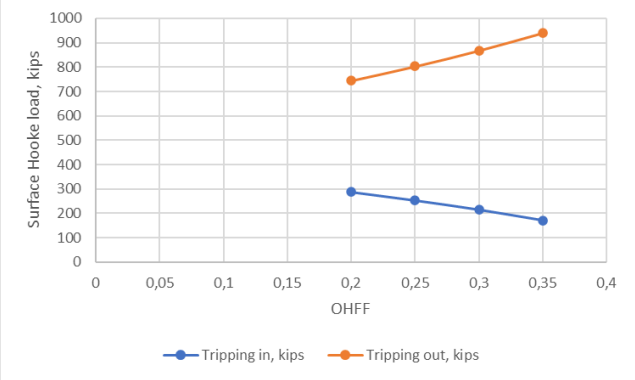

Figure 4. Effect of OHFF on the HKL.

Figure 4 highlights the effect of the open-hole friction factor (OHFF) on the Hook load (HKL) during tripping in and tripping out operations. The results demonstrate that variations in OHFF lead to significant changes in the HKL, with distinct trends for the two operations. Specifically, increasing the OHFF results in a higher HKL during tripping out but a lower HKL during tripping in. This behavior is primarily attributed to the role of drag forces and their directional influence on the HKL in these operations.

As OHFF increases, the frictional drag force acting on the drillstring also increases. However, the direction of this drag force relative to the HKL determines its impact. During tripping in, the drag force opposes the motion of the string and acts in a direction opposite to the HKL. Consequently, the drag force is subtracted from the HKL, leading to a reduction in the measured HKL as the OHFF increases. Conversely, during tripping out, the drag force aligns with the motion of the string and acts in the same direction as the HKL. This alignment adds to the HKL, causing it to increase with higher OHFF values.

Quantitative analysis of the results shows that an increase in OHFF by a factor of 0.05 results in a -13.4% change in HKL during tripping in and a +8% change during tripping out. These substantial changes underscore the sensitivity of HKL to friction factor variations and the critical need for accurate determination of OHFF. Inaccurate calculations or assumptions regarding friction factors can lead to significant deviations between predicted and actual HKL values. Such discrepancies can create serious operational challenges, including excessive mechanical stresses that may lead to breaking the drill line, pulling the rig inward, or even parting the drillstring.

The influence of OHFF on HKL is not uniform across different wellbore sections. In vertical wellbore sections, where contact between the drillstring and the wellbore wall is minimal, the effect of OHFF on HKL is relatively small. However, as the wellbore deviates and the hole angle becomes more critical, the increased contact between the drillstring and the wellbore wall amplifies the impact of friction. This increased contact results in a more pronounced influence of OHFF on the HKL, making accurate friction factor estimation even more essential in deviated and extended-reach wells.

4.4. Effect of tripping speed on the HKL

Tripping speeds affects the dynamic force acting on the drillstring. During tripping operations, the speed at which the string is pulled or lowered in the wellbore must be properly calculated to avoid diverse problems. One such problem is surge and swab. It has been discovered that the magnitude of tripping speeds also impacts the HKL as illustrated in Figure 5.

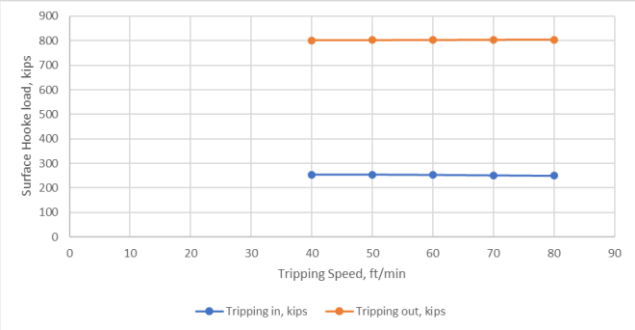

Figure 5. Effect of tripping speed on the HKL.

Figure 5 demonstrates the effect of tripping speeds on the HKL during tripping in and tripping out operations. The results indicate that variations in tripping speed lead to changes in HKL magnitude, with opposing trends for the two operations. Specifically, increasing the tripping speed reduces the HKL during tripping in but increases it during tripping out. This behaviour is driven by the combined effects of swab and surge pressures and dynamic frictional drag, which vary with the speed of the tripping operation.

During tripping out, the upward movement of the drillstring generates swab pressures, which are associated with a reduction in bottomhole pressure caused by the displacement of fluid. As tripping speeds increase, these swab pressures rise, creating additional resistance to the upward motion of the string. This increased resistance contributes to a higher HKL during tripping out, reflecting the additional force required to overcome both the string's weight and the swab-induced drag.

Conversely, during tripping in, the downward motion of the string generates surge pressures, which are caused by the displacement of fluid toward the bottomhole. These pressures act to reduce the apparent weight of the string, thereby lowering the HKL. The effect becomes more pronounced at higher tripping speeds, as the increased surge pressures further decrease the HKL magnitude.

In addition to swab and surge pressures, dynamic frictional drag also plays a role in the variation of HKL with tripping speeds. As the tripping speed increases, the dynamic component of friction becomes more significant. This increased drag force adds to the HKL during tripping out but reduces it during tripping in, amplifying the observed trends.

Despite these effects, the overall impact of tripping speeds on HKL is relatively small. Quantitative analysis reveals that for every 10 ft/min increase in tripping speed, the HKL changes by an average of -0.37% during tripping in and +0.08% during tripping out. These marginal variations suggest that while tripping speeds influence HKL, their effect is secondary to factors such as friction factors and mud weight.

4.5. Effect of tripping rotary speeds (RPM)

Rotating the drillstring can lead to significant impact on the HKL when tripping. The primary reason why the drillstring is rotated is to alter frictional forces and dynamic loads which is critical to the overall axial loads on the drillstring. When the speed of the trip is purely translational, frictional drag arises due to sliding contact between the drillstring and the walls of the wellbore. However, when the string is rotated during tripping, some of the sliding friction is converted to rolling friction reducing the overall drag. The effect of RPM on the HKL during tripping is illustrated in Figure 6.

Figure 6 illustrates the impact of rotary speed on the Hook load (HKL) during tripping in and tripping out operations, revealing opposing trends. As the rotary speed of the drillstring increases, the HKL during tripping in increases, while it decreases during tripping out. These variations can be attributed to the interplay between sliding and rolling friction under dynamic conditions.

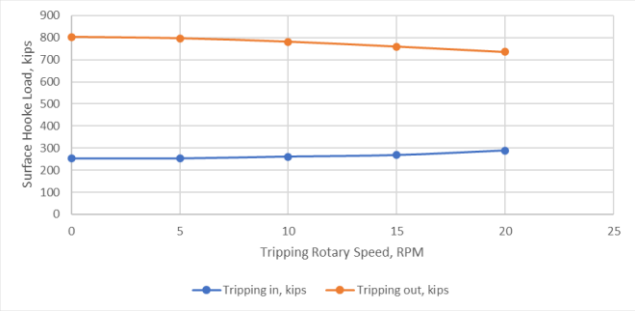

Figure 6. Effect of RPM on the HKL during tripping.

Friction is the primary drag force encountered when the drillstring and the wellbore, are in contact. Under static conditions, the drag force is determined by the coefficient of static friction and the normal reaction force. However, in dynamic conditions, the coefficient of static friction transitions to the coefficient of dynamic friction, which is inherently lower. This reduction in friction as motion begins is the key factor influencing the HKL during tripping operations.

During tripping out, the HKL corresponds to the tensile force required to pull the drillstring upward against gravity and drag forces. As the rotary speed increases, the transition from static to dynamic friction reduces the drag force encountered. This reduction lowers the tensile force required, resulting in a decrease in HKL. The drillstring effectively moves more freely as the rotary speed rises, reducing resistance and improving operational efficiency.

In contrast, during tripping in, the HKL corresponds to the apparent compressive force needed to lower the string into the wellbore. The compressive load decreases as rotary speed increases because of the reduced drag force under dynamic friction. However, since compression is a negative load relative to the HKL, the reduction in compressive force effectively results in an increase in the net HKL. In other words, as less compressive force opposes the HKL, the observed HKL magnitude grows. Increasing rotary speed provides operational benefits by reducing drag during tripping out, which can minimize wear on the drillstring and improve efficiency. However, the increase in HKL during tripping in due to reduced compressive resistance warrants attention, as it may affect load distribution along the drillstring and exacerbate buckling risks under specific conditions.

4.6. Result of RSM modelling

The results of the RSM modelling are presented and discussed in this section. RSM model was developed by fitting the simulation sensitivity data obtained from WellPlan. Among several regression models tested, the quadratic model demonstrated the highest fit to the actual data for tripping in while the linear model demonstrated the highest fit to the input data for tripping out HKL. These modes where being selected for their superior prediction accuracy.

Equation 5 is the quadratic model generated by RSM for tripping in HKL

$$HKL_{trippingin}\ (kips) = 249.2\ - 0.191667\mathrm{A} - 43.7917\mathrm{B} - 9.8\mathrm{C}\ +\ 29.7167\mathrm{D}\ +\ 3.2\mathrm{AB}\ +\ 0.45\mathrm{AC}\ +\ 1.825\mathrm{AD} - 5\mathrm{BC}\ +\ 11.475\mathrm{BD} - 5.75\mathrm{CD} - 3.4875\mathrm{A}^2\ +\ -12.0625\mathrm{B}^2\ +\ 2.55\,\mathrm{C}^2\ +\ 2.4\mathrm{D}^2 \quad (5)$$

Equation 6 is the linear model generated by RSM for tripping out HKL

$$HKL_{trippingout}\ (kips) = 805.948\ - 3.65833\mathrm{A}\ +\ 54.3583\,\mathrm{B}\ +\ 11.7333\mathrm{C}\ - 45.9667\mathrm{D} \quad (6)$$

where variables A, B, C, and D represent mud weight, friction factor (OHFF), tripping speed, and RPM respectively, this equation can be utilized to predict the response for given levels of each factor.

The levels are specified in the original units of each factor, both for the input parameters and the response variables to achieve accurate predictions, To assess the significance of the model coefficients, Analysis of Variance (ANOVA) was conducted. Table 5 and Table 6 summarize the ANOVA results and fit metrics for HKL responses. Table 5 include degrees of freedom, mean square values, F-values, and p-values. In Table 5, the p-values are smaller than 0.0001, and the high F-values indicate that the models are statistically significant.

The fit summary statistics corresponding to the ANOVA, including the coefficient of determination (R^2), adjusted R^2, predicted R^2, Adequate precision, standard deviation, and coefficient of variation (C.V), are presented in Table 6.

Table 5. ANOVA statistics for the performance of the models.

Source	Degree of freedom		Mean square		F-Value		p-Value	
	HKL tripping in	HKL tripping out	HKL tripping in	HKL tripping out	HKL tripping in	HKL tripping out	HKL tripping in	HKL tripping out
Model	14	4	2630.53	15656.45	57.16	250.56	<0.0001	<0.0001
Residual	14	4	46.02	62.49				
Cor Total	28	28						

Table 6 demonstrates the robust predictive capability of the model for HKL tripping in and HKL tripping out, with R^2, Adjusted R^2, and predicted R^2 values of 0.9828, 0.9656, and 0.9010, respectively for tripping in and 0.9766, 0,9727, and 0.9634 respectively for tripping out. The small difference between the adjusted R^2 and predicted R^2 (less than 0.2) indicates good agreement between the actual data and the model-predicted response. Typically, R^2 values above 0.9 indicate a strong fit between experimental and predicted outcomes. The low coefficient of variation (CV) at 2.77% and 0.98% for tripping in and tripping out respectively further highlights the reliability of the results.

Table 6. Fit summary statistics for the models.

Fit parameter	HKL tripping in	HKL tripping out
R2	0.9828	0.9766
Adjusted R^2	0.9656	0.9727
Predicted R^2	0.9010	0.9634
Adeq precision	30.13	61.13
Std dev	6.78	7.9
C.V. %	2.77	0.98

Table 7 shows the predicted values generated by the RSM models for each input variable alongside the actual output data. It emphasizes the strong correlation observed between the actual experimental results and the predictions made by the RSM models.

Table 7. Actual and predicted results for HKL for tripping out and tripping in.

Run	Mud Weight, ppg	OHFF	Tripping Speed, ft/min	Tripping Rotary Speed, RPM	HKL tripping in, kips		HKL tripping out, kips	
					Actual Value	Predicted Value	Actual Value	Predicted Value
1	10.5	0.35	80	20	186.2	181.1	879	872.04
2	10.5	0.35	60	20	221.7	210.7	840.3	848.57
3	10.5	0.25	70	10	261	265.09	790.8	797.56
4	10.5	0.3	80	30	266.6	268.32	773.3	771.71
5	10.5	0.25	60	20	288.9	288.28	738.4	739.86
6	10.8	0.3	70	10	219	216.38	848.1	848.26
7	10.5	0.3	70	20	249.2	249.2	805.2	805.95
8	10.5	0.3	70	20	249.2	249.2	805.2	805.95
9	10.2	0.25	70	20	281.3	280.83	756.5	755.25
10	10.8	0.3	60	20	258	257.42	783.4	790.56
11	10.2	0.3	60	20	259.1	258.7	790.6	797.87
12	10.5	0.3	80	10	220.7	220.38	857.3	863.65

Run	Mud Weight, ppg	OHFF	Tripping Speed, ft/min	Tripping Rotary Speed, RPM	HKL tripping in, kips		HKL tripping out, kips	
					Actual Value	Predicted Value	Actual Value	Predicted Value
13	10.5	0.3	70	20	249.2	249.2	805.2	805.95
14	10.2	0.35	70	20	174.3	186.85	866.3	863.96
15	10.2	0.3	70	30	279.3	276.2	757.1	763.64
16	10.8	0.35	70	20	185.4	192.87	858.4	856.65
17	10.5	0.25	80	20	273.4	278.68	764.3	763.32
18	10.5	0.3	60	10	223.2	228.48	844.7	840.18
19	10.5	0.3	70	20	249.2	249.2	805.2	805.95
20	10.5	0.3	70	20	249.2	249.2	805.2	805.95
21	10.5	0.35	70	30	242.3	236.94	799.6	814.34
22	10.2	0.3	70	10	228.3	220.41	855.9	855.57
23	10.5	0.3	60	30	292.1	299.42	773.3	748.25
24	10.8	0.25	70	20	279.6	274.05	749.7	747.93
25	10.5	0.25	70	30	304.3	301.57	711.6	705.62
26	10.8	0.3	80	20	239.6	238.72	815.1	814.02
27	10.8	0.3	70	30	277.3	279.46	750.3	756.32
28	10.5	0.35	70	10	153.1	154.55	920	906.27
29	10.2	0.3	80	20	238.9	238.2	822.5	821.34

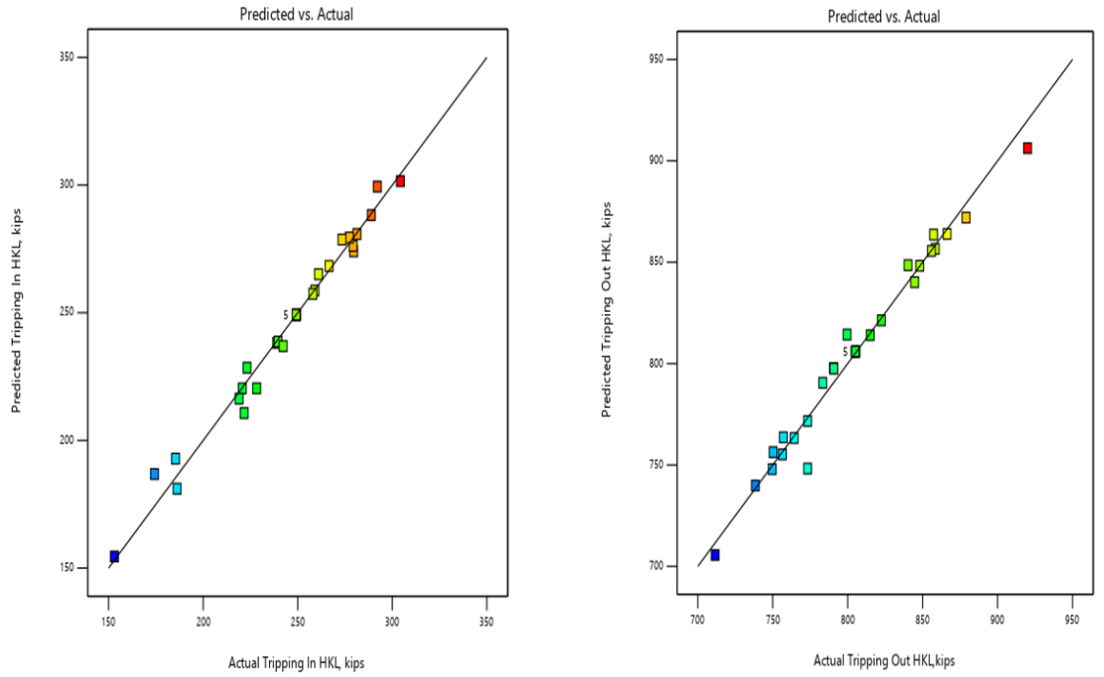

Figure 7. Parity plot of actual vs. predicted values of a) tripping in HKL b) tripping out HKL.

Figure 7 shows the actual vs. predicted response for the quadratic regression model. Figure 7 depict parity plots illustrating the relationship between the actual and predicted water conent

of dry gas. This figures demonstrate that the actual and predicted output responses closely align around the 45-degree line, indicating strong regression and agreement between the two datasets. Thus, there exists an acceptable level of agreement between the actual data (simulated sensitivity dataset) and the predicted responses from the RSM model.

4.7. Interaction response of parameters using 3D plots and contour plots

Figure 8 and Figure 9 illustrate the 3D response surface plot and contour plots from the RSM model depicting the interaction between independent variables and tripping in HKL. These plots visually represent how changes in the independent variables influence the response providing insights into their mutual interactions

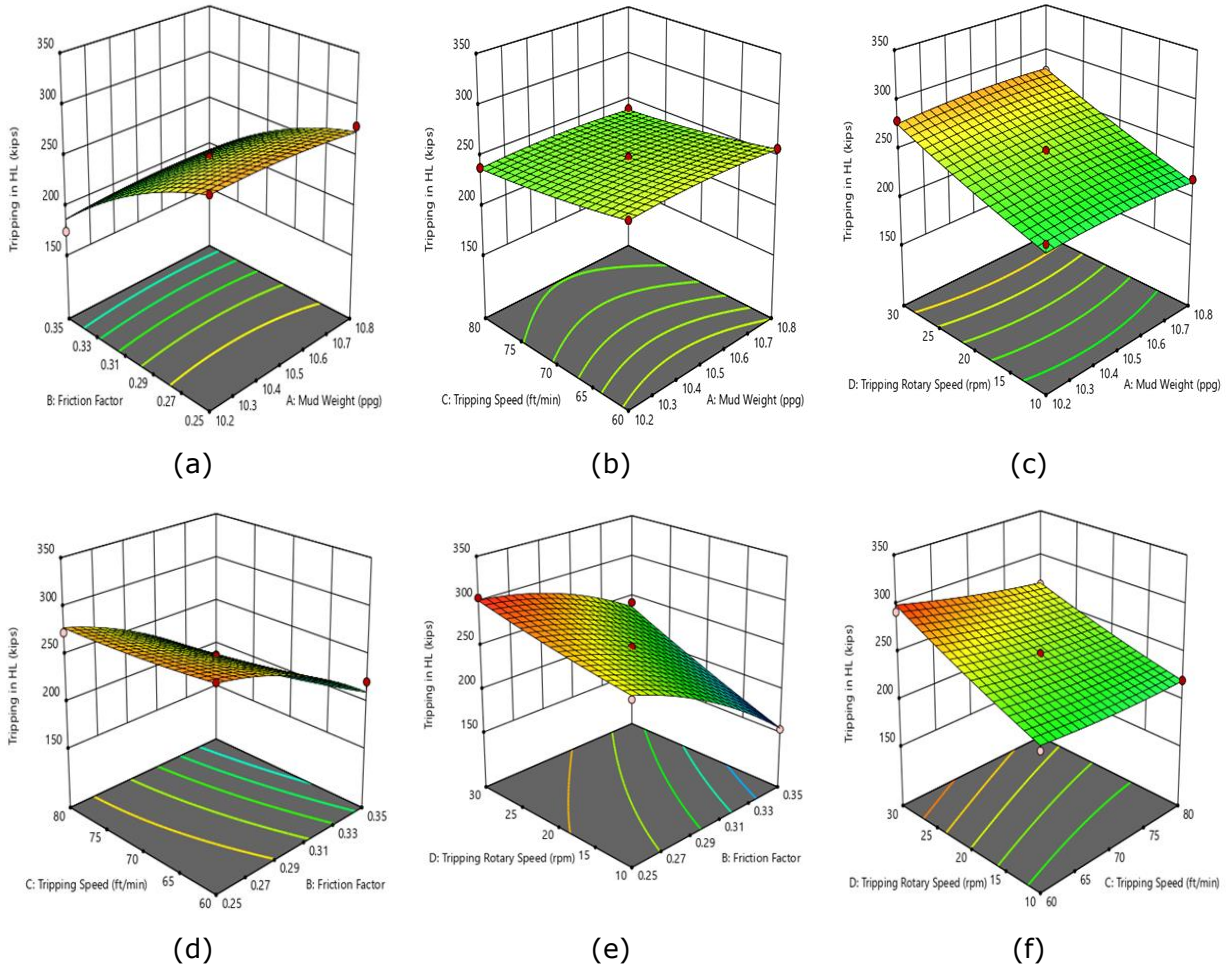

Figure 8. 3D response surface plots for tripping in HKL from RSM.

The 3D response surface plot for tripping in HKL is shown in Figure 8a-f, while Figure 9a-f shows the contour plots. Both the 3D surface plots and the contour plots are used to make analysis of the interactions between the independent variables and the response.

Figure 8a and Figure 9a shows the interactive effect of mud weight and friction factor (OHFF) on the tripping in HKL. It can be observed that mud weights decrease the tripping in HKL at higher OHFF. Moreover, both mud weight and OHFF inversely impacts the HKL as their increase led to corresponding decrease in the values of the HKL. However, it should be noted that the effect of mud weight on the tripping in HKL was quite moderate. Figure 8b and Figure 9b shows the interactive effects of mud weight and tripping speed (ft/min) on the HKL. It can be seen that at increasing the mud weight led to slight decrease in the HKL at higher tripping speeds. Moreover, both the mud weight and tripping speeds impact the HKL inversely although

the effect was very slightly. Figure 8c and Figure 9c depicts the interactive effect between mud weight and rotary speeds of trips on the HKL. It can be observed that increasing the RPM causes the tripping in HKL to increase at lower mud weights. However. Increasing the mud weights at constant RPM led to decrease in the tripping in HKL

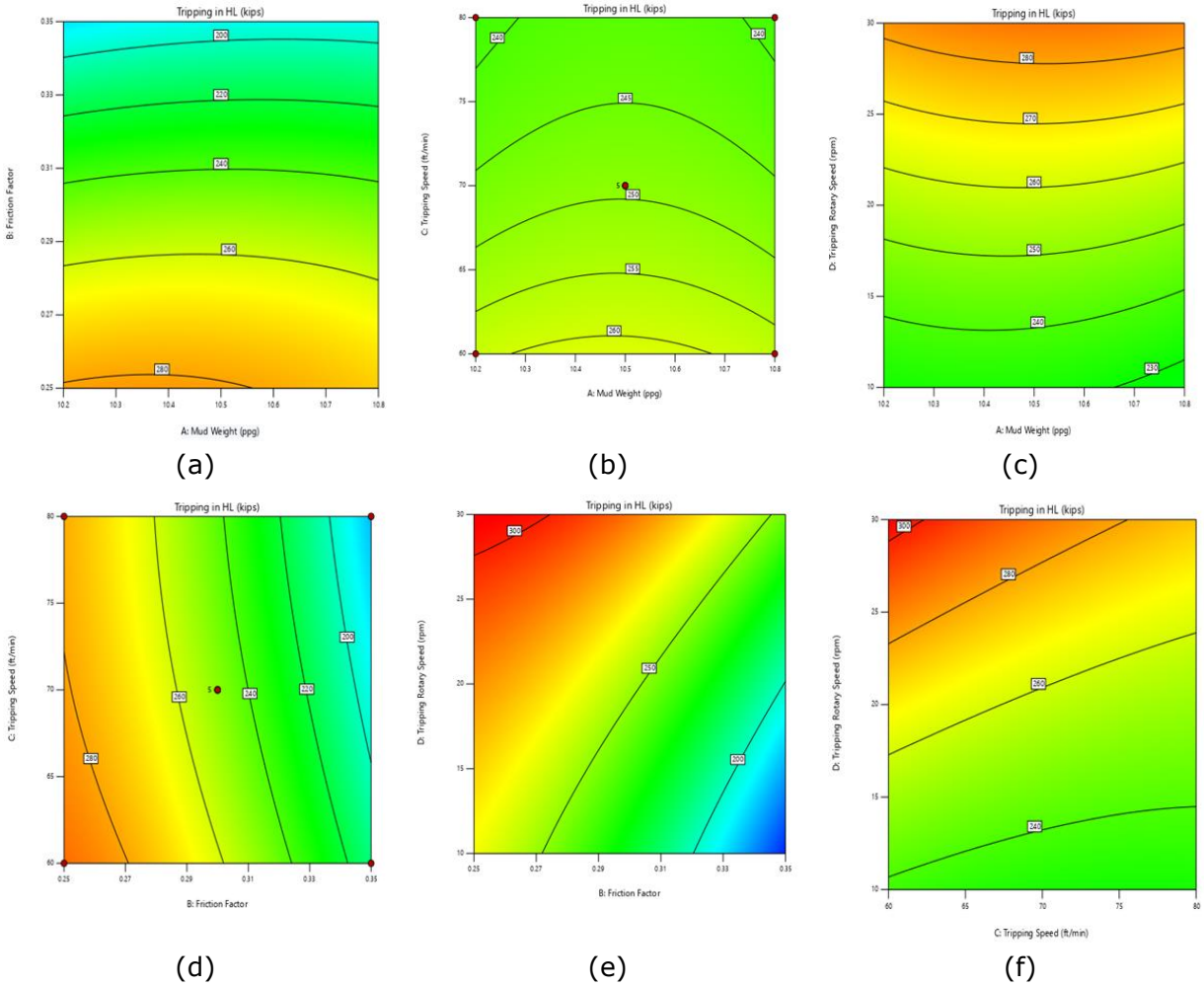

Figure 9. Contour plots for tripping in HKLs from RSM.

The interaction between friction factors (OHFF) and tripping speeds contributes to variation of the tripping in HKL as shown in figure 8d and 9d. It can be observed that increasing the OHFF led to decrease in the tripping in HKL at higher tripping speeds (ft/min). Moreover, both the friction factor and the tripping speed impacts the tripping in HKL inversely. Figure 8e and Figure 8e depict the interactive effect of friction factor and rotary speed of the trip on the tripping in HKL. It was observed that at higher RPM, the tripping in HKL increased at lower OHFF. Nevertheless, when the RPM was kept constant, the tripping in HKL decreased as OHFF was increased. Figure 8f and Figure 9f illustrates the interactive effects of tripping speed (ft/min) and the rotary speed of trip (RPM) on the tripping in HKL. At lower tripping speed (ft/min), the tripping in HKL increased as RPM was increased. However, when the RPM was kept constant, increasing the tripping speed (ft/min) decreased the tripping in HKL.

There was no two-parameter interaction for tripping out HKL with the input parameters because the representative model was linear.

5. Conclusion

A comprehensive modelling of Hook loads in drilling of extended reach wells has been conducted. Hook loads have been investigated when analyses torque and drag for tripping in and

tripping out operations. Accurate Hook load determination was critical to prevent problems in drilling such as breaking the drill line, pulling the rig in, or parting the drillstring. WellPlan software was used to model the drillstring torque and drag with specific focus on the Hook load. Sensitivity analyses were carried out to assess the impact of key parameters including mud weight, open-hole friction factors, tripping speed, and rotary speed (RPM) on the Hook load of the drillstrings. RSM modelling was applied to explore and quantify the interactions between these parameters, providing a robust framework for understanding their combined effects on HKL dynamics. This modelling effort offers valuable insights for optimizing tripping operations and mitigating risks associated with load mismanagement in complex wellbore environments. Result showed that tripping operations in exhibited distinct variations in HKL behaviour depending on the direction of movement. During tripping out, HKL tends to be higher due to drag forces aligning with the load direction, whereas during tripping in, drag opposes the load, leading to comparatively lower HKL values. Mud weight also plays a significant role, with higher weights reducing HKL by enhancing buoyancy forces, particularly during tripping out. Additionally, open-hole friction factors (OHFF) strongly influenced HKL dynamics. Higher OHFF values resulted in increased HKL during tripping out due to increased friction, while during tripping in, the same factors reduced HKL by counteracting the load more effectively.

Tripping speeds and rotary motion further influence HKL. Higher tripping speeds increased dynamic pressures such as surge and swab, causing HKL to increase during tripping out and decrease during tripping in. Rotary speed (RPM) contributes by transforming frictional drag from sliding to rolling, effectively lowering HKL during tripping out but slightly increasing it during tripping in. The RSM modelling demonstrated that the quadratic model for tripping in HKL and the linear model for tripping out HKL achieved excellent predictive accuracy and were used to represent the design space respectively. For tripping out, the R^2, adjusted R^2, and predicted R^2 values were 0.9766, 0.9727, and 0.9634, respectively, while for tripping in, these values were 0.9828, 0.9656, and 0.9010. Statistical validation through ANOVA and fit summary statistics confirmed the robustness and reliability of these models, showing minimal discrepancies between observed and predicted data. These insights are critical for optimizing tripping operations and HKLs during drilling operation. By strategically manipulating factors such as mud weight, friction control, and rotary motion, drilling teams can mitigate risks associated with helical buckling and string yielding, improve operational safety, and achieve more efficient drilling performance. This understanding of HKL dynamics is essential for developing robust strategies in extended reach and challenging well environments.

References

[1] Farab AE, Shahbazi K, Hashemi A, Shahbazi A. New Method for Predicting Casing Wear in Highly Deviated Wells Using Mud Logging Data. Research Square. 2021. https://doi.org/10.21203/rs.3.rs-1036212/v1

[2] Lin Y, Deng K, Xing Q. A new crescent-shaped wear equation for calculating collapse strength of worn casing under uniform loading. J Pressure Vessel Technol. 2015;137(3):031201. https://doi.org/10.1115/1.4029588

[3] Al-haj AKB, Al-Daow AB, Abdulrahman OA, Mubarak MMY. Modelling of Torque and Drag in Extended Reach Drilling Using Landmark Software (Case Study: a well in Field X, Block 2B). Bachelor's Project, Sudan University of Science and Technology, Sudan; 2015.

[4] Neamah HA, Alrazzaq AA. Torque and Drag Forces Problems in Highly Deviated Oil Well. Iraqi J Chem Petrol Eng. 2018; 19(3): 19-31.

[5] Samuel R, Zhang Y. Tortuosity: The Rest of the Hidden Story. IADC/SPE Conference & Exhibition. The Hague; 2018. SPE-194167-MS.

[6] Deng S, Liu Y, Jiang P, Zhu S, Tao L, He Y. Simulation and experimental study of deepwater subsea wellhead-shallow casing deflection considering system mass force. Ocean Eng. 2019; 187: 106222.

[7] Ohia NP, Ekwueme ST, Achumba GI, Okereke NO, Nwankwo IV, Nnwanwe OI. Analysis of Critical Buckling Loads For Tool-Jointed Drillstrings in Deviated Wellbores. SPE Nigeria Annual Int Conf Exhibition. 2021; D021S008R005.

[8] Sanchez A, Brown CF, Adams W. Casing centralization in horizontal and extended reach wells. SPE/EAGE European Unconventional Resources Conf Exhibition. 2012; SPE-150317.

[9] Huang W, Gao D, Liu Y. Mechanical model and optimal design method of tubular strings with connectors constrained in extended-reach and horizontal wells. J Petrol Sci Eng. 2018; 166: 948-61.
[10] Xiaohua Z, Ke K, Jiawei A. Calculation and analysis of dynamic drag and torque of horizontal well strings. Nat Gas Ind B. 2019; 6: 183-90. https://doi.org/10.1016/j.ngib.2018.08.004
[11] Wang X, Chen P, Ma T, Liu Y. Modelling and experimental investigations on the drag reduction performance of an axial oscillation tool. J Nat Gas Sci Eng. 2017; 39: 118-32.
[12] Mirhaj SE, Kaarstad SE, Aadnoy BS. Torque and drag Modelling: Soft String vs Stiff String. IADC/SPE Drilling Conf Exhibition. Abu Dhabi, UAE; 2016.
[13] Nwonodi RF, Adali F, Tswenma T. Predicting Drillstring Buckling. Am J Eng Res. 2017; 6(5): 301-11.
[14] Orji BA, Anwana ME. Design and Analysis of Drilling String Buckling in Directional Wells. Int J Curr Eng Technol. 2017; 7(6): 2062-9.
[15] Eric C, Skadsem HJ, Kluge R. Accuracy and correction of hook load measurements during drilling operations. SPE/IADC Drilling Conf Exhibition. 2015; D021S010R005.
[16] Luke GR, Juvkam-Wold HC. Determination of True Hook Load and Line Tension Under Dynamic Conditions. SPE Drill Complet. 1993; Texas, USA.
[17] Adzokpe J. Hook-load Measurements made with a Draw-works as a Function of Sensor Placement and Dynamic Conditions. MSc Thesis. Univ of Stavanger, Norway; 2014.
[18] Sánchez L, Lapo M, Zorrilla O. Torque and drag analysis of a drill string using Sequential Monte Carlos methods. J Petrol Sci Eng. 2019;173:1-12. https://doi.org/10.1016/j.petrol.2018.09.039
[19] Li X, Gao D, Lu B. Study on modified maximum extension length prediction model for horizontal wells considering differential sticking. J Petrol Sci Eng. 2019; 183: 1-13. https://doi.org/10.1016/j.petrol.2019.106371
[20] Huang W, Gao D. Analysis of drilling difficulty of extended-reach wells based on drilling limit theory. Petrol Sci. 2022;19:1099-1109. https://doi.org/10.1016/j.petsci.2021.12.030
[21] Zhang Y, Samuel R. Dilemma: When to Use Soft String and Stiff String Torque and Drag Models. SPE Annu Tech Conf Exhibition. Calgary, Canada; 2019.
[22] Li X, Gao D, Zhou Y. General approach for the calculation and optimal control of the extended-reach limit in horizontal drilling based on the mud weight window. J Nat Gas Sci Eng. 2016; 35: 964-79. https://doi.org/10.1016/j.jngse.2016.09.049
[23] Wylie R, Standefer J, Anderson J, Soukup I. Instrumented Internal Blowout Preventer Improves Measurements for Drilling and Equipment Optimization. SPE/IADC Drilling Conf Exhibition. 2013; SPE-163475.
[24] Liu Y, Ma T, Chen P, Yang C. Method and apparatus for monitoring of downhole dynamic drag and torque of drill-string in horizontal wells. J Petrol Sci Eng. 2018;164:320-32. https://doi.org/10.5897/JPGE2022.036410.1016/j.petrol.2018.01.077
[25] Ohia NP, Ekwueme ST, Achumba G, Okereke NU, Nwankwo IV, Nwanwe OI. A Comparative Study of Soft String Vs Stiff String Models Application in Torque and Drag Analysis. Nigeria Annu Int Conf Exhibition. Lagos, Nigeria; 2021.
[26] Kerunwa A, Anyadiegwu CI, Asuquo IK, Okereke NU, Udeagbara SG, Ekwueme ST. Investigation of the viscous fluid effect on torque and drag modelling in highly deviated wells. Journal of Petroleum and Gas Engineering, 2024; 16(1): 1-16. https://doi.org/10.5897/JPGE2022.0364
[27] Wang XM, Yao XM. Vibration Technologies for Friction Reduction to Overcome Weight Transfer Challenge in Horizontal Wells Using a Multi-scale Friction Model. Lubricants. 2018; 6: 53.
[28] Nobandegani MS, Birjandi MRS, Darbandi T, Khalilipour MM, Shahraki F, Mohebbi-Kalhori D. An industrial Steam Methane Reformer optimization using response surface methodology. J Nat Gas Sci Eng. 2016; 36: 540-9.
[29] Yusuf DD, Upahi EJ, Yusuf HO. Multi-Response Optimization of Planting Process of a Seed Ridge Planter using Response Surface Methodology (RSM). Arid Zone J Eng Technol Environ. 2023; 19(4): 897-910.
[30] Yusuf M, Farooqi AS, Alam MA, Keong LK, Hellgardt K, Abdullah B. Response surface optimization of syngas production from greenhouse gases via DRM over high performance Ni–W catalyst. Int J Hydrogen Energy. 2022; 47(72): 31058-71.
[31] Fazaelizadeh M. Real time torque and drag analysis during directional drilling. PhD dissertation, Univ of Calgary; 2013.
[32] Chukwuemeka AO, Amede G, Alfazazi U. A Review of Wellbore Instability During Well Construction: Types, Causes, Prevention And Control. Petroleum & Coal, 2017; 59(5): 590-610.

[33] Alwasitti AA, Al-Zubaidi NS, Salam M. Enhancing Lubricity of Drilling Fluid using Nanomaterial Additives. Petroleum & Coal, 2019; 61(3): 467-479.
[34] Kerunwa A, Anyadiegwu CI. Overview of the Advances in Casing Drilling Technology. Petroleum & Coal. 2015; 57(6): 661-675.

To whom correspondence should be addressed: Stanley Toochukwu Ekwueme, Department of Petroleum Engineering, Federal University of Technology, Owerri, Nigeria, E-mail: *stanleyekwueme@yahoo.com*